Viscoelastic Dynamic Response of Asphalt Pavement in Long Slope Sections

Yuanyuan Gao[1,2], Shuai Dong[3], Han Xiao[3], Nkosilathi lovewell Hlupo[3], Zhi Liu[3*]

[1] Hebei Province Engineering Research Center for Harmless Synergistic Treatment and Recycling of Municipal Solid Waste, Yanshan University, No. 438 West Hebei Avenue, 066004, Qinhuangdao, Hebei, China
[2] Key Laboratory of Green Construction and Intelligent Maintenance for Civil Engineering of Hebei Province Yanshan University, No. 438 West Hebei Avenue, 066004, Qinhuangdao, Hebei, China
[3] School of Civil Engineering & Mechanics, Yanshan University, No. 438 West Hebei Avenue, 066004, Qinhuangdao, Hebei, China
* Corresponding author, e-mail: liuzhi@stumail.ysu.edu.cn

Abstract

To deeply understand the performance of asphalt pavement in long slope sections, the object of this paper is to obtain the viscoelastic dynamic response of asphalt pavement in long slope sections considering interface bonding conditions. An asphalt pavement model is built, and then for solving the problem, the Laplace-Hankel transformation is used to transfer the partial differential equations to the ordinary differential equations. Transfer matrices are adopted to present the relationship of stress and displacement between the pavement surface and any pavement depth, and a special transfer matrix characterizes the interface bonding condition. By this method, the analytical solution of the stress and displacement at any pavement position is received. After that, an example of asphalt pavement in a long slope section is introduced considering the distribution of stress and displacement, the magnitude of the horizontal load, and the interface bonding strength. The horizontal vehicle load affects the distribution of shear stress τ_{rz} in the pavement. The interface bonding strength is more important in long slope sections than in any other normal section of asphalt pavement.

Keywords

asphalt pavement, long slope sections, imperfect interface, Laplace-Hankel integral, transfer matrix

1 Introduction

The load imposed on the pavement mainly comes from vehicles and, based on the form of wheels rolling the road, it contains both vertical and horizontal loads. Compared with the vertical load of a vehicle, the horizontal load caused by slid friction is usually smaller in normal sections of the road and is always neglected in pavement design and pavement simulation. However, in some special sections of the road, e.g., long slope, bus stations, crossroads, etc., the vehicle brake, stop, and frequently restart, which causes a larger horizontal load than in normal sections of the road. In these sections, the interface between layers of asphalt pavement is usually not very well, and the pavement surface is prone to cause diseases such as slippage and congestion, which significantly impairs the service life and driving comfort of the road. Under these conditions, the horizontal load caused by the vehicle starting and braking can't be ignored [1]. To better understand the mechanical behavior of the asphalt pavement in these sections, we focus on the performance of the typical asphalt pavement section, the long slope section. Therefore, firstly an effective model for simulating the working conditions of an asphalt pavement during its whole service life should be built, which involves the constitutive relation of the asphalt layer and describing the character of the interface bonding condition between two layers. And then an efficient approach is necessary to resolve the issue.

Asphalt mixture consists of bitumen binder, aggregate, fine aggregate, additives, etc.; it is typically a viscoelastic material. The researchers employed several constitutive laws and methods to simulate the behavior of viscoelastic materials [2–5], such as the Kelvin-Voigt viscoelastic model [6], Generalized Maxwell rheological model [7], Kelvin, Maxwell, Vanderpoel, and Burgers models are commonly used to present the performance of asphalt layers in analytical methods [8–9]. Some experts conducted excellent work in this field as well. Darabi et al. [10], proposed

a coupled nonlinear viscoelastic (VE)-viscoplastic (VP)-hardening-relaxation (HR) constitutive model to characterize the behavior of asphalt mixtures and then validated that the VE-VP-HR model can capture the response of asphalt mixtures subjected to various loading paths by experimental data. Karimi et al. [11], presented a large-deformation thermodynamic-based framework and got a large deformation, time-dependent viscoplastic constitutive relationship for predicting the compaction degree of asphalt concrete materials under laboratory and field. The Helmholtz free energy and rate of energy dissipation functions were used in their research to derive rate-dependent constitutive relationships of asphalt concrete during compaction. Numerical algorithms associated with the proposed constitutive relationship were implemented in the finite element (FE) code ABAQUS by the user material subroutine UMAT to calibrate the constitutive model. Zhu and Sun [12] derived a viscoelastic–viscoelastic damage constitutive model based on irreversible thermodynamics theory to describe the triaxial creep and triaxial constant strain rate compression tests and predict the time-dependent response of asphalt mixtures under various compression loading conditions. The Burgers model is still one of the most widely used constitutive relations for characterizing the properties of asphalt layers [13–14]. However, Burgers constitutive relation has one weakness, which can't describe the solidification procedure of asphalt mixture. Because the coefficient that characterizes the permanent deformation of the material is constant, it can only display the directly proportional relationship between permanent deformation and time. However, the viscous flow deformation of the asphalt mixture decreases as the service time of the pavement increases. To overcome this drawback, Xu and Zhu [15] proposed a modified Burgers model, and in this model, the viscosity coefficients of the dashpot in the modified Maxwell parameter aren't a constant, and it is modified as an exponential function of time. In this paper, we adopt the modified Burgers model to describe the behavior of the asphalt layer, and a more detailed introduction of the modified Burgers model is in Section 2.

Asphalt pavement structure with a semi-rigid base is usually adopted in China, and the modified bitumen is used as a binder between the two layers. Even though the binder improves the bonding strength, sometimes the bonding condition can't be considered completely continuous for the materials of the asphalt layer and the base course have different characteristics. The performance of asphalt pavement is affected by the bonding conditions between two layers [16–17]. Therefore, the performance of bonding conditions should be considered in building asphalt pavement models. For simulating the behavior of asphalt pavement, bonding conditions are generally modeled by a specific layer, cohesion zone element, and coulomb model [18–20]. Using the Coulomb friction model, Wang and Ma [21] simulated the bonding condition between the adjacent layers of semi-rigid base asphalt pavement by contact element and target element. They found that disengaging area between the asphalt concrete layer and the base layer can negatively affect the strain responses of asphalt pavement, especially at the higher temperature, and it can also weaken the asphalt pavement performance with the increase of the disengaging area. In Xu et al. [22] study, by the discrete-element model, asphalt pavement was established to discuss the effects of temperature changes of the interlaminar bonding layer on the mechanical responses of asphalt pavement. Their research shows that lower temperature increases the continuity of asphalt pavement layers, reducing the compressive stress in the upper layer. On the contrary, higher temperature weakens the interlaminar bond, increasing the horizontal tensile stress in the upper layer and at the interlaminar interface. Using the calculation software Ever Stress FE, characterize the bonding conditions of the asphalt pavement structure by setting specially processed 16-node elements at layer interfaces and introducing the interface stiffness, which is defined as the ratio of the shear stress at the top and bottom of the interface element to the relative shear displacement [23]. For the analysis method, the classical Goodman law [24] is used for deriving the constitutive relation of the interface because, on one side, it can describe the performance of the interface. On the other side, it makes the procedure of the formula derivation concise. Therefore, the Goodman model is adopted in this paper to characterize the performance of the bonding condition of the asphalt pavement.

Based on the current achievement, in this paper, building an asphalt pavement model considering the viscoelastic property of the asphalt layer and the bonding strength of the interface under the vertical and horizontal vehicle load can get a more realistic simulation of the asphalt pavement in long slope sections. On the other hand, the analytical method is more convenient and accurate to obtain the mechanical behaviors of the pavement. Because changing parameters and multiple matrices can simulate the pavement in different conditions, rather than building several models for each condition.

The outline of this paper is that in Section 2, the model of asphalt pavement considers the incompletely continuous bonding condition under vertical and horizontal vehicle load. The procedure of analytical solution derivation is presented in Section 3. To illustrate the application of the methods proposed in this paper, an example is calculated in Section 4, and the factors which influent the trend of the viscoelastic dynamic response of the pavement are analyzed in this section. The last part is the conclusion in Section 5.

2 Model of asphalt pavement in long slope sections
2.1 Modified Burgers model
Asphalt pavement comprises several layers, asphalt layer, base course, sub-base, subgrade, etc. Due to the properties of bitumen, the asphalt layer presents viscoelastic features, and the other layers are usually considered elastic materials for building asphalt pavement models.

In this paper, the modified Burgers model is selected to characterize the constitutive relation of the asphalt layer, as shown in Fig. 1 [15]. Based on the classical Burgers model, a Maxwell model, and a Kelvin model in series, Xu [15] modified the Maxwell model, replacing the viscosity coefficient η_1 with an exponential function of t in Eq. (1), for describing the procedure of solidification of asphalt mixture,

$$\eta_1(t) = Ae^{Bt} ,$$ (1)

where A and B are the coefficients of dashpot in the modified Maxwell model.

There is no modification in the Kelvin model, so the constitutive relation of the Kelvin model can be expressed as

$$\sigma_k = \eta_2 \frac{d\varepsilon_k}{dt} + E_2 \varepsilon_k ,$$ (2)

where σ_k and ε_k are the stress and strain of the two parallel elements, respectively. η_1 is the coefficient of the dashpot in the Kelvin model and E_2 is the spring's stiffness.

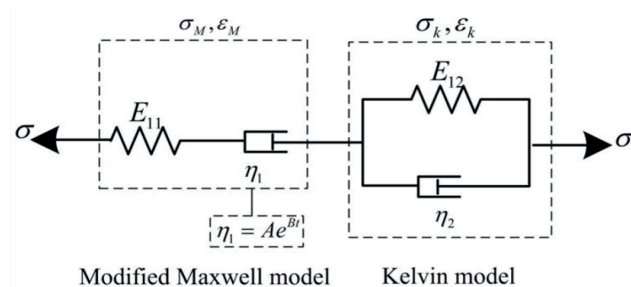The normal stress of the spring element in the Maxwell model is

Fig. 1 Modified Burgers model

$$\sigma_1 = E_1 \varepsilon_1 ,$$ (3)

where E_1 is stiffness of the spring in the modified Maxwell model and ε_1 is strain of this spring.

For the dashpot, the stress can be expressed as

$$\sigma_2 = \eta_1 \frac{d\varepsilon_2}{dt} = Ae^{Bt} \frac{d\varepsilon_2}{dt} ,$$ (4)

where σ_2 and ε_2 are the stress and strain of the dashpot in the modified Maxwell model.

Based on the property of the series element that, $\sigma_M = \sigma_1 = \sigma_2$, $\varepsilon_M = \varepsilon_1 = \varepsilon_2$, the constitution relation can be obtained

$$\frac{\sigma_M}{Ae^{Bt}} + \frac{1}{E_1} \frac{d\sigma_M}{dt} = \frac{d\varepsilon_M}{dt} .$$ (5)

In terms of the series of modified Maxwell model and Kelvin model,

$$\sigma = \sigma_K = \sigma_M ,$$ (6)

$$\varepsilon = \varepsilon_M + \varepsilon_K .$$ (7)

The constitutive relation of the modified Burgers model could be proposed as

$$(\frac{E_{12} - B\eta_2}{Ae^{Bt}})\sigma + (\frac{E_{12}}{E_{11}} + \frac{\eta_2}{Ae^{Bt}} + 1)\frac{d\sigma}{dt} + \frac{\eta_2}{E_{11}} \frac{d^2\sigma}{dt^2}$$
$$= E_{12} \frac{d\varepsilon}{dt} + \eta_2 \frac{d^2\varepsilon}{dt^2} ,$$ (8)

where E_{11} and E_{12} are elastic parameters in Maxwell and Kelvin model, respectively. η_2 is the viscosity coefficient in the Kelvin model. σ is the normal stress and ε is the normal strain.

2.2 Interface bonding conditions
Former research points out that the bonding condition between two pavement layers significantly affects the deformation of asphalt pavement under traffic load [25–27], and the bonding condition isn't usually continuous. Especially in the section of crossroads, bus stations, long slopes, etc., the bonding strength deteriorates with the increase of service time of pavement. The Goodman model [28] is selected for characterizing the bonding conditions between the pavement layers shown in Fig. 2.

It reflects the relationship between shear stress and relative horizontal displacement at the interlayer interface. The constitutive relation can be expressed as
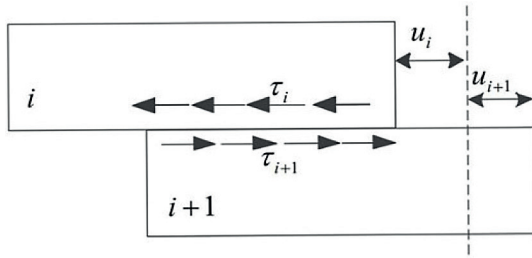
Fig. 2 Schematic diagram of Goodman model

$$\tau_{zr(i+1)} = \tau_{zri} = K_i \Delta u , \qquad (9)$$

where $\tau_{zr(i+1)}$ and τ_{zri} are the shear stress of the $(i + 1)^{\text{th}}$ layer and the i layer, respectively. u_{i+1} and u_i are the displacement of the $(i + 1)^{\text{th}}$ layer and the ith layer. K_i is the adhesion coefficient, which represents the bonding strength. $K_i \to \infty$ means that the interface between two layers is almost completely continuous. On the contrary, $K_i \to 0$ presents the two layers that could move free horizontally. Δu is the relative horizontal displacement $\Delta u = u_{i+1} - u_i$.

2.3 Vehicle load
In the long slope sections of the road, because of the vehicle braking and starting, the vertical load and the horizontal load should be considered. Therefore, the vehicle load is simplified as both vertical and horizontal parts, as shown in Fig. 3. Apart from vehicle braking and starting load, the component of vehicle gravity along the surface of pavement contributes to the horizontal load as well. However, it is smaller than the horizontal load caused by vehicle braking and starting, because the angle of the slope in high-grade road is usually less than 5–6 degree. Therefore, in this model, the horizontal load caused by the vehicle gravity is neglected.

Considering the vibration of vehicles driving on the road, the continuous semi-sinusoidal load is selected for the vertical load. Based on Deng and Li [29] research, for considering the maximum shear stress, the horizontal load with one direction could be assumed as the symmetry load with z axle, and semi-rectangular wave load is selected for the horizontal load. The vertical and horizontal load are expressed as [30].

$$P(t) = \begin{cases} p[H(t) - H(t - T_d)]\sin^2(\dfrac{\pi}{T_d})t & (r < R) \\ 0 & (r > R) \end{cases}, \qquad (10)$$

$$g(t) = \begin{cases} F_{xb\max}[H(t) - H(t - T_d)] & (r < R) \\ 0 & (r > R) \end{cases}, \qquad (11)$$
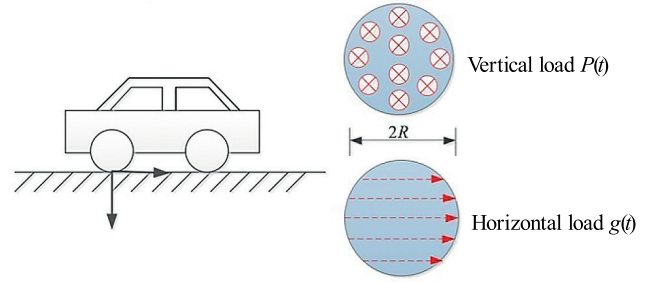

Fig. 3 The schematics of vehicle load

where $H(t)$ is a step function, t is the loading time, and T_d is the loading period. $F_{xb\max}$ is the maximum braking load of the vehicle, $F_{xb\max} = \varphi p$, φ is the road friction coefficient and p is the vertical load amplitude.

At the infinite vertical distance of the road $z \to \infty$, the stress and displacement are assumed as

$$u(r,\infty,t) = 0, w(r,\infty,t) = 0, \\ \tau_{zr}(r,\infty,t) = 0, \sigma_z(r,\infty,t) = 0. \qquad (12)$$

And then, considering the viscoelastic behaviors of the asphalt layer, the asphalt model with an imperfect interface under braking vehicle load is shown in Fig. 4

3 Resolution of the asphalt pavement model
The dynamic equilibrium equations of an axisymmetric problem in polar coordinates presented by displacement can be expressed as

$$[\lambda(t) + G(t)]\frac{\partial e(r,z,t)}{\partial r} + G(t) \\ \left(\nabla^2 u(r,z,t) - \frac{u(r,z,t)}{r^2}\right) = \rho \frac{\partial^2 u(r,z,t)}{\partial t^2}, \qquad (13)$$

$$[\lambda(t) + G(t)]\frac{\partial e(r,z,t)}{\partial z} + G(t)\nabla^2 w(r,z,t) \\ = \rho \frac{\partial^2 w(r,z,t)}{\partial t^2}, \qquad (14)$$

where $\lambda(t)$ and $G(t)$ are Lame constant, $\lambda(t) = \mu E(t)/(1+\mu)(1-2\mu)$, $G(t) = E(t)/2(1+\mu)$, $e(r, z, t)$ is the volume deformation. $e(r,z,t) = \partial u(r,z,t)/\partial r + u(r,z,t)/r + \partial w(r,z,t)/\partial z$, ∇^2 is a Laplace operator, $\nabla^2 = \partial^2/\partial r^2 + \partial/(r\partial r) + \partial^2/\partial z^2$. u and w represent the horizontal and vertical displacements, respectively; ρ is the density of pavement material and t is the time variable.

For getting the solution of Eqs. (13) and (14) and the relationship of stress and displacement in different layers of the pavement, two auxiliary equations coming from Hooke's law were introduced as Eqs. (15) and (16).
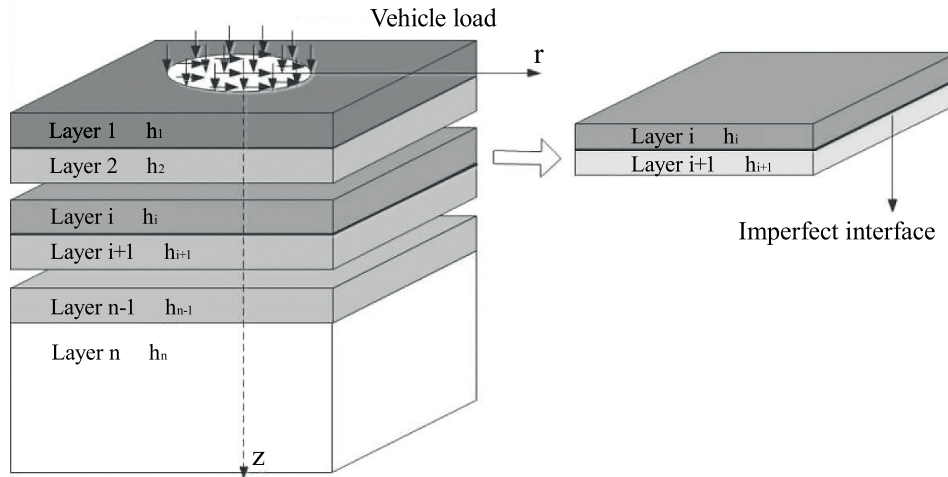
Fig. 4 Calculation model of asphalt pavement structure under vehicle braking condition

$$\sigma_z(r,z,t) = \lambda(t)e(r,z,t) + 2G(t)\frac{\partial w(r,z,t)}{\partial z} \tag{15}$$

$$\tau_{zr}(r,z,t) = G(t)(\frac{\partial u(r,z,t)}{\partial z} + \frac{\partial w(r,z,t)}{\partial r}), \tag{16}$$

where σ_r, σ_θ and σ_z represent stresses in the r, θ and z directions, respectively; τ_{zr} is the shear stress.

Equations (13)–(16) are all partial differential equation with respect to two variables, t and r. Compare with ordinary differential equation, they are more challenging to be solved directly. For transforming partial equation into ordinary equation, Laplace-Hankel transformation is adopted in Eqs. (13)–(16). Firstly, Laplace integral transformation is applied to the time variable t in Eqs. (13)–(16), and then by simplifying these complex equations, which can be obtained as

$$\overline{\tau}_{zr}(r,z,s) = G(s)\left(\frac{\partial \overline{u}(r,z,s)}{\partial z} + \frac{\partial \overline{\omega}(r,z,s)}{\partial r}\right), \tag{17}$$

$$\overline{\sigma}_z(r,z,s) = \lambda(s)e(r,z,s) + 2G(s)\frac{\partial \overline{\omega}(r,z,s)}{\partial z}, \tag{18}$$

$$\left[\lambda(s) + G(s)\right]\frac{\partial \overline{e}(r,z,s)}{\partial r} + G(s)$$
$$\left(\nabla^2 \overline{u}(r,z,s) - \frac{\overline{u}(r,z,s)}{r^2}\right) = \rho s^2 \overline{u}(r,z,s), \tag{19}$$

$$\left[\lambda(s) + G(s)\right]\frac{\partial \overline{e}(r,z,s)}{\partial z} + G(t)\nabla^2 \overline{\omega}(r,z,s)$$
$$= \rho s^2 \overline{\omega}(r,z,s). \tag{20}$$

Equations (17)–(20) are still a set of partial differential equations with one variable r. Then Hankel integral transformation is performed on the variable r in Eqs. (17)–(20). After simplification, it can be obtained,

$$\frac{d\tilde{\overline{u}}(\xi,z,s)}{dz} = \xi\tilde{\overline{w}}(\xi,z,s) + \frac{1}{a(s)}\tilde{\overline{\tau}}_{zr}(\xi,z,s), \tag{21}$$

$$\frac{d\tilde{\overline{w}}(\xi,z,s)}{dz} = -\frac{\mu\xi}{1-\mu}\tilde{\overline{u}}(\xi,z,s) + \frac{1}{b(s)}\tilde{\overline{\sigma}}_z(\xi,z,s), \tag{22}$$

$$\frac{d\tilde{\overline{\tau}}_{zr}(\xi,z,s)}{dz} = \left[\rho s^2 + \frac{2a(s)}{(1-\mu)}\right]\tilde{\overline{u}}(\xi,z,s) + \frac{\mu\xi}{(1+\mu)}\tilde{\overline{\sigma}}_z(\xi,z,s), \tag{23}$$

$$\frac{d\tilde{\overline{\sigma}}_z(\xi,z,s)}{dz} = \rho s^2 \tilde{\overline{w}}(r,z,s) - \xi\tilde{\overline{\tau}}_{zr}(\xi,z,s), \tag{24}$$

where $a(s) = \frac{E(s)}{2(1+\mu)}, b(s) = \frac{(1-\mu)E(s)}{(1+\mu)(1-2\mu)}$ $a(s)$ and $b(s)$ are functions of variables related to material properties in the Laplace transformation domain. If the material is considered as linear elasticity, then $a(s)$ and $b(s)$ are constants. In the model shown in Fig. 4, the asphalt layer is considered viscoelastic, and the other layers are linear elastic.

The modified Burgers model is used to characterize the constitutive relation of pavement asphalt layer material. By Laplace integral transformation of the time variable t in the constitutive Eq. (8) of the modified Burgers model, the expression of its viscoelastic operator in the Laplace domain can be obtained

$$E(s) = \frac{\sigma(s)}{\varepsilon(s)} =$$
$$\frac{sA(s+B)E_{11}(E_{12}+s\eta_2)}{sA(s+B)(E_{11}+E_{12}+s\eta_2) + E_{11}\left[-B^2E_{12} - s^2B\eta_2 + B^3\eta_2 + s(sE_{11}+\eta_2)\right]} \tag{25}$$

That is, the mathematical expression of the material properties of the asphalt layer is obtained; bring $E(s)$ into $a(s)$ and $b(s)$, we can get the specific expression of $a(s)$ and $b(s)$. Equations (21)–(24) can be expressed uniformly in matrix form

$$\frac{d\tilde{\bar{X}}(\xi,z,s)}{dz} = [\psi]\tilde{\bar{X}}(\xi,z,s), \tag{26}$$

where

$$[\psi] = \begin{bmatrix} 0 & \xi & \dfrac{1}{a(s)} & 0 \\ -\dfrac{\mu\xi}{1-\mu} & 0 & 0 & \dfrac{1}{b(s)} \\ c(s) & 0 & 0 & \dfrac{\mu\xi}{(1+\mu)} \\ 0 & \rho s^2 & -\xi & 0 \end{bmatrix},$$

$$c(s) = \rho s^2 + \frac{E(s)}{(1+\mu)(1-\mu)}.$$

The solution of Eq. (26) can be obtained based on modern control theory [31], and it can be expressed as

$$\tilde{\bar{X}}(\xi,z,s) = \exp[z\psi(\xi,s)]\tilde{\bar{X}}(\xi,0,s), \tag{27}$$

where $\exp[z\psi(\xi, s)]$ characterizes the transfer relationship between stresses and displacements at different locations in the same material and $\exp[z\psi(\xi, s)]$ is a fourth-order matrix. If $\exp[z\psi(\xi, s)]$ is expressed in $[T]$, then Eq. (27) can be rewritten as

$$\tilde{\bar{X}}(\xi,z,s) = [T]\tilde{\bar{X}}(\xi,0,s). \tag{28}$$

Because the asphalt pavement structure is a half-space multi-layers structure system, if the interlayer is considered to be completely continuous, the stresses and displacements of $z = h$ at the bottom of the layer i and top of a layer $i + 1$ are equal, namely

$$\begin{bmatrix} \tilde{\bar{u}}(\xi,h,s) \\ \tilde{\bar{w}}(\xi,h,s) \\ \tilde{\bar{\tau}}_{zr}(\xi,h,s) \\ \tilde{\bar{\sigma}}_z(\xi,h,s) \end{bmatrix}_{i+1} = \begin{bmatrix} \tilde{\bar{u}}(\xi,h,s) \\ \tilde{\bar{w}}(\xi,h,s) \\ \tilde{\bar{\tau}}_{zr}(\xi,h,s) \\ \tilde{\bar{\sigma}}_z(\xi,h,s) \end{bmatrix}_i. \tag{29}$$

Then the stresses and displacements at any depth of the pavement can be expressed as (layer $i + 1$)

$$\tilde{\bar{X}}(\xi,z,s)_{i+1} = [T_{i+1}][T_i]...[T_2][T_1]\tilde{\bar{X}}(\xi,0,s). \tag{30}$$

In the section of crossroad, bus station, long longitudinal slope, etc., the bonding strength between pavement layers degenerates during its' service life and can't be regarded as a completely continuous boundary condition.

In this paper, the Goodman model is used to characterize the imperfect interface between asphalt pavement layers. Equation (28) can be rewritten to

$$u_{i+1} = \frac{\tau_{zi}}{K_i} + u_i. \tag{31}$$

Bring Eq. (31) into (29), and we can get

$$\begin{bmatrix} \tilde{\bar{u}}(\xi,h,s) \\ \tilde{\bar{w}}(\xi,h,s) \\ \tilde{\bar{\tau}}_{zr}(\xi,h,s) \\ \tilde{\bar{\sigma}}_z(\xi,h,s) \end{bmatrix}_{i+1} = [T_{ci}] \begin{bmatrix} \tilde{\bar{u}}(\xi,h,s) \\ \tilde{\bar{w}}(\xi,h,s) \\ \tilde{\bar{\tau}}_{zr}(\xi,h,s) \\ \tilde{\bar{\sigma}}_z(\xi,h,s) \end{bmatrix}_i, \tag{32}$$

where the specific form of $[T_{ci}]$ is

$$[T_{ci}] = \begin{bmatrix} 1 & 0 & \dfrac{1}{K_i} & 0 \\ 0 & 1 & 0 & 0 \\ 0 & 0 & 1 & 0 \\ 0 & 0 & 0 & 1 \end{bmatrix}. \tag{33}$$

Therefore, the displacement and stress at any depth of layer $i + 1$ in asphalt pavement with an imperfect interface can be expressed as

$$\tilde{\bar{X}}(\xi,z,s)_{i+1} = [T_{i+1}][T_{ci}]...[T_2][T_1]\tilde{\bar{X}}(\xi,0,s), \tag{34}$$

where T_{ci} is a special transformation matrix.

If there are more layers and several discontinuous interfaces in the pavement, we only need to give the index i a larger value and insert the special transfer matrix into a general transfer matrix sequence. For instance, if the interfaces between the first and second layers and the ith and $(i + 1)$th layers are discontinuous, Eq. (34) can be modified as

$$\tilde{\bar{X}}(\xi,z,s)_{i+1} = [T_{i+1}][T_{ci}]...[T_2][T_{c1}][T_1]\tilde{\bar{X}}(\xi,0,s). \tag{35}$$

This is the advantage of the method proposed in this paper for there is no need to build a new model to calculate the dynamic response of asphalt pavement with more layers and more imperfect interfaces.

Based on the boundary conditions of the model shown in Fig. 4, the analytical solution of stress and displacement at any position of the pavement is gained in the Laplace and Hankel transformation domain. By introducing the boundary conditions into Eq. (34) and using inverse transformation of numerical integration [32], the numerical solution of any pavement position in a physical domain can be obtained.

4 Results and discussion

To investigate the factors that affect the dynamic response of asphalt pavement, an asphalt pavement with imperfect bonding conditions under vertical and horizontal vehicle loads is introduced. The asphalt pavement is simplified to a three-layer structure, and Fig. 5 shows the asphalt pavement. According to the author's previous research [33],
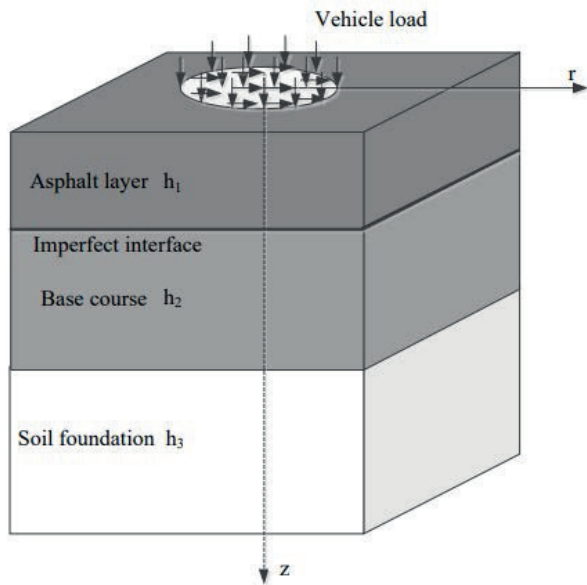
Fig. 5 Three-layers asphalt pavement model

Table 1 Geometrical and mechanical parameters of the pavement structure

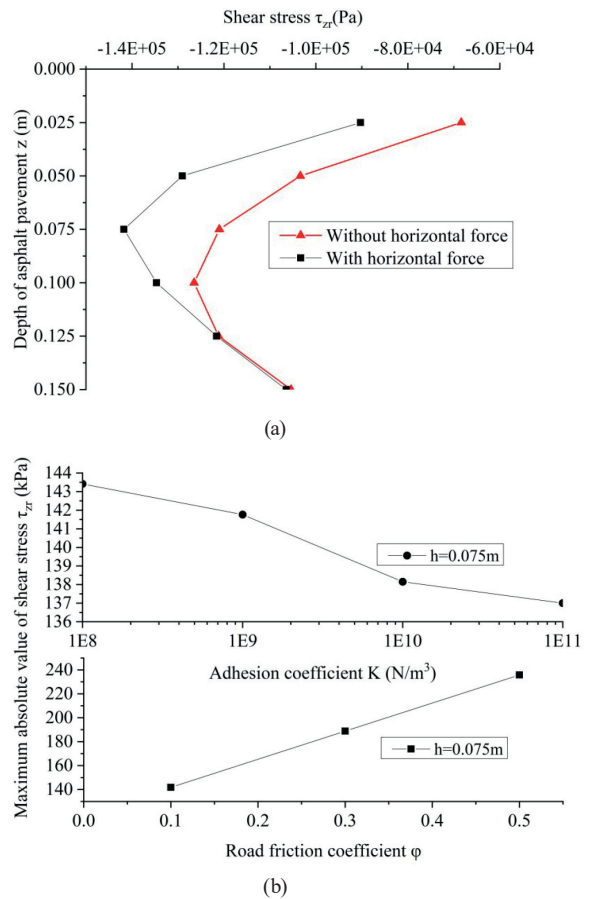| Pavement structure	Asphalt layer	Base course	Soil foundation
Thickness /m	0.18	0.35	—
elastic modulus /MPa	1000	—	—
elastic modulus /MPa	100	—	—
viscoelastic coefficient /(MPa·s)	105	—	—
viscoelastic coefficient	1010	—	—
viscoelastic coefficient	0.01	—	—
elastic modulus/MPa	—	1500	100
Density /(kg/m³)	2100	2000	1900
Poisson ratio	0.25	0.25	0.35

Fig. 6 (a) Comparison of shear stress calculation results with and without horizontal load, (b) Calculation results of the maximum absolute value of shear stress with different bonding conditions and different horizontal loads

the bonding condition between the asphalt layer and the base course of the asphalt pavement has the most significant influence on the dynamic response of the pavement. Table 1 illustrates the geometric and mechanical parameters of the pavement. The vertical load amplitude is $p = 0.7$ MPa, $R = 0.15$ m, and the load period is $T_d = 32$ ms. The vertical displacement, normal vertical stress, and shear stress are calculated with different bonding conditions and horizontal loads, and the results are shown in Figs. 6–8.

Fig. 6(a) shows the shear stress of asphalt pavement in different positions with and without horizontal force, and Fig. 6(b) focuses on the influence of both the interface bonding strength and horizontal force on the shear stress τ_{rz} in $h = 0.075$ m. Comparing the two different lines in Fig. 6(a), the results illustrate that the horizontal load enlarges the shear stress greatly and changes its distribution in the pavement. The maximum shear stress emerges closer to the pavement surface, considering the horizontal load. In the top one, Fig. 6(b), the shear stress sharply decreases with $K = 10^8 - 10^{10}$ N/m³, and then with the value of K increase, the shear stress increases slightly. It also means that the interface bonding strength affects the stress value in the pavement. However, if the bonding strength is large enough, it can be seen as a perfect interface. The bottom one of Fig. 6 illustrates that the horizontal force affects the shear stress a lot, and the maximum absolute value of shear stress increase as the road friction coefficient φ increase linearly. Therefore, in the design stage of pavement in long slope sections, the horizontal vehicle load should be and the quality of the instruction is very essential for ensuring the strength of interface bonding.

Figs. 7(a), (b), and (c) present the vertical displacement of the pavement considering the positions, the magnitude of the horizontal load, and the interface bonding strength, respectively. In Fig. 7(a), the value of displacement decreases as the position is far from the surface of the pavement in the depth direction, and the horizontal load slightly affects the displacement on the surface of

the pavement. The results shown in Fig. 7(c) demonstrate again that the horizontal load contributes little to the displacement. On the contrary, the interface bonding strength
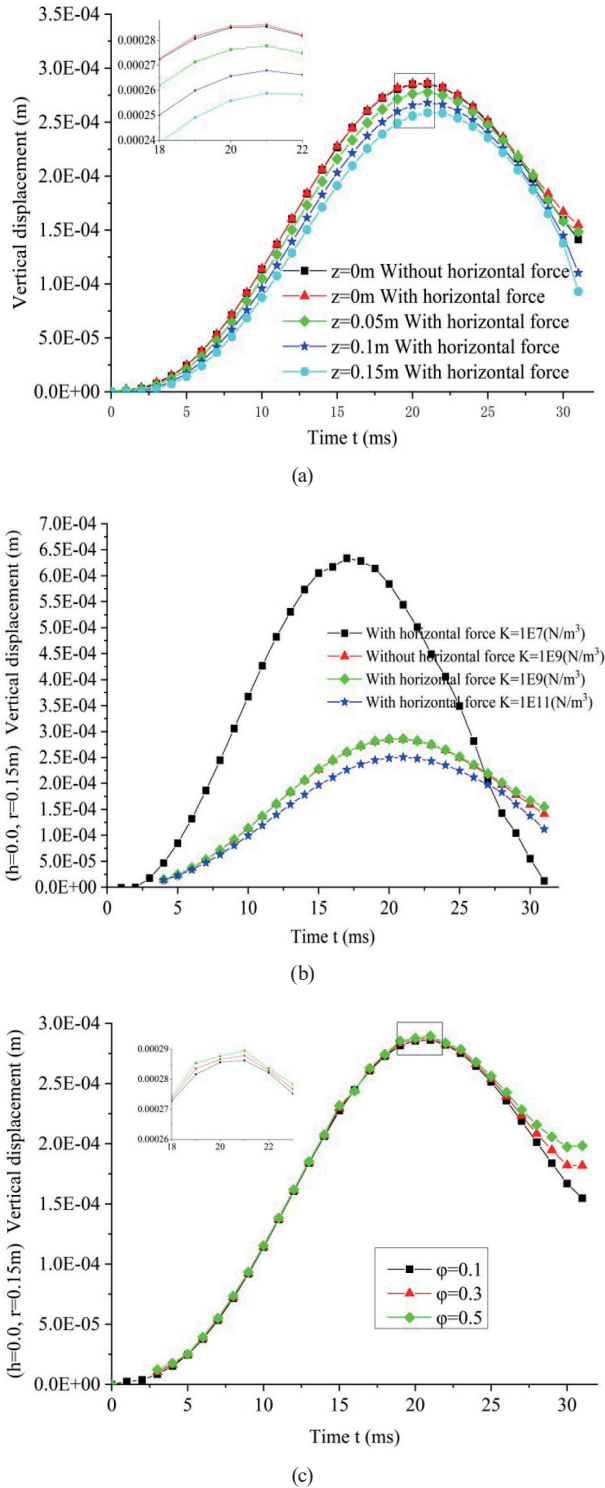

(a)

(b)

(c)

Fig. 7 (a) Comparison of displacement calculation results in different depths with and without horizontal load, (b) Comparison of displacement calculation results with different bonding conditions, (c) Comparison of displacement calculation results with different horizontal loads

has significant effect on the variation of the vertical displacement of the pavement shown in Fig. 7(b). Especially on the condition of $K = 10^7$ N/m³, the value of displacement rises dramatically, and with the interface bonding strength increase, the value of displacement goes down moderately. The displacement and shear stress of the pavement has the same variable tendency on the changing of interface bonding strength. It means that the horizontal load contributes to the displacement indirectly, because the horizontal load affects the stress distribution in the pavement, and then increased stress causes the decrease of the interface bonding strength.

The normal stress σ_z in different positions of asphalt pavement is calculated with and without horizontal load, and the results are shown in Fig. 8(a). Figs. (b) and (c) present the calculation results of the normal stress σ_z considering the different bonding conditions and different horizontal forces, respectively. In Fig. 8(a), at the same position $h = 0.5$ m, comparing the two different lines which present the calculation results of normal stress σ_z with and without horizontal load, respectively, it is evident that the horizontal load leads to the increase of the normal stress σ_z and it also can be seen that the normal stress σ_z decrease as the position deepens in the pavement. Compared with shear stress and vertical displacement, the adhesion coefficient contributes very little to the vertical stress σ_z, as shown in Fig. 8(b). On the contrary, the normal σ_z stress increase as the road friction coefficient increases considerably. These can explain why rutting emerges in the long slope sections more likely, for the normal stress σ_z increase with the horizontal load increase.

5 Conclusions

In this paper, a calculation model of asphalt pavement under vertical and horizontal vehicle load is established for understanding the influence of horizontal load in long slope road sections on the dynamic response of asphalt pavement, considering the interface bonding conditions. In the procedure of derivation for the analytical solution of the model, the method of Laplace-Hankel integral transformation is used to transfer partial differential equations to ordinary differential equations, and then a transformation matrix is introduced to characterize the behavior of the imperfect interface. An example of asphalt pavement is presented to validate the method proposed in this paper. The main factors that affect the dynamic response of asphalt pavement in long slope sections are analyzed, and the following conclusions are obtained:
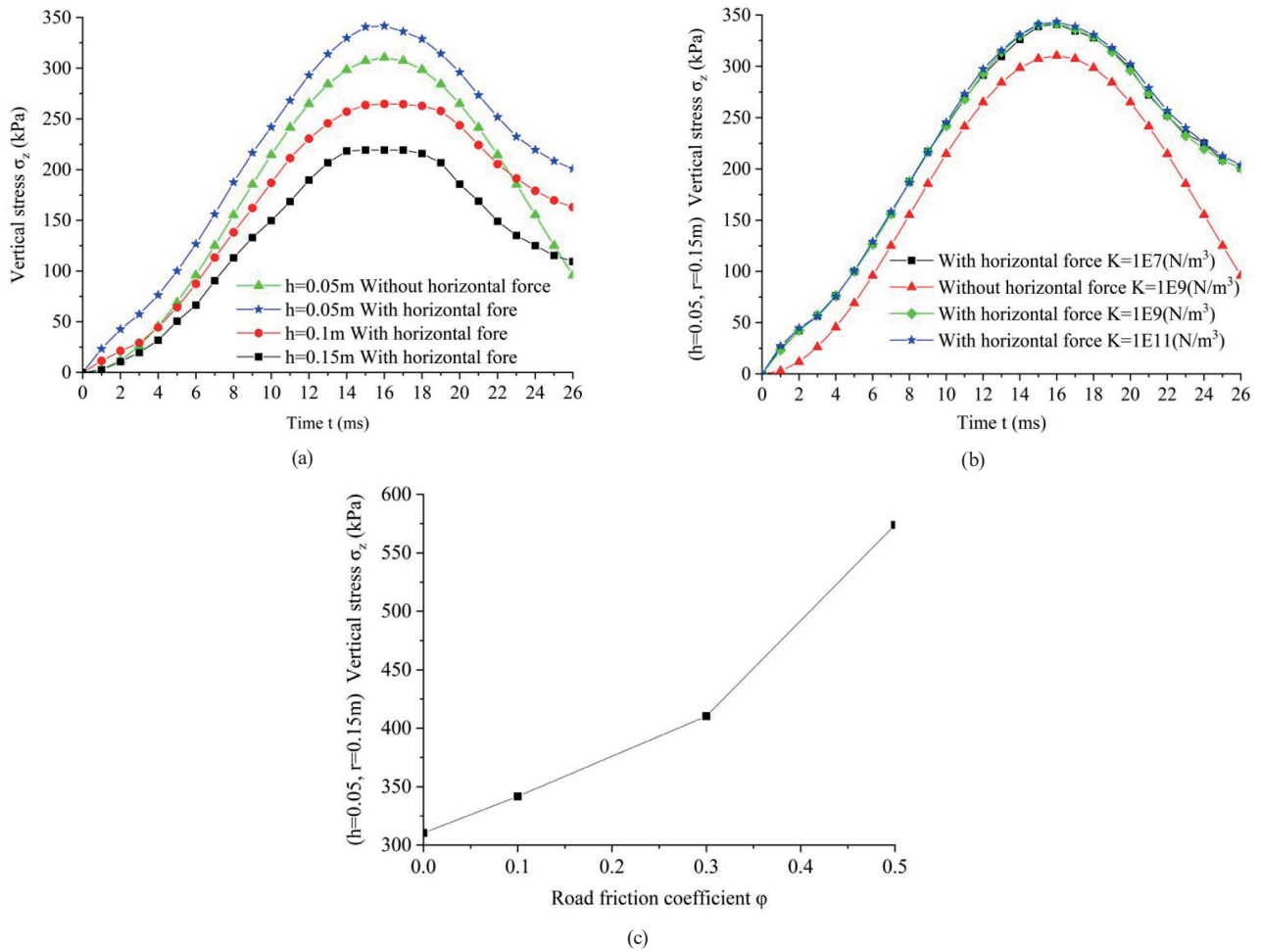
Fig. 8 (a) Comparison of vertical stress in different depths of asphalt pavement with and without horizontal load, (b) Comparison of vertical stress with different adhesion coefficient, (c) Comparison of vertical stress with different road friction coefficient

(1) The interface bonding condition between the asphalt layer and the base course of asphalt pavement contributes considerably to the value of shear stress and displacement. As the bonding strength degenerates, the shear stress and displacement at the edge of the traffic load in different depths increase largely. By contrast, as the adhesion coefficient K increase, the shear stress and displacement decrease slightly. Therefore, if the adhesion coefficient K is large enough, the stress and displacement will not change. On that condition, the interface can be seen as perfect.

(2) In the long slope sections of road, the horizontal vehicle load enlarges the value of vertical displacement, shear stress τ_{rz}, and normal stress σ_z at the edge of vehicle load in different depth of asphalt pavement and affect the distribution of the stress, especially the shear stress τ_{rz}, and the normal stress σ_z. During the service period of asphalt pavement in long slope sections, the horizontal load increases the shear stress τ_{rz}, the enlarged shear stress τ_{rz} enhances the risk of deterioration of the interface bonding strength, and then the decreased interface bonding strength enlarges the shear stress τ_{rz}, which is a vicious circle. Therefore, in long slope sections of asphalt pavement, the vertical vehicle load and the interface bonding strength should be paid more attention together.

References

[1] Guo, J., Yang, S., Sun, Y., Chao, Z., Yang, R., Cheng, H. "Analysis of shear stress and rutting performance of semirigid base asphalt pavement on steep longitudinal slope", Advances in Civil Engineering, 2021, 4445653, 2021.
https://doi.org/10.1155/2021/4445653

[2] Wollny, I., Hartung, F., Kaliske, M. "Numerical modeling of inelastic structures at the loading of steady state rolling", Computational Mechanics, 57, pp. 867–886, 2016.
https://doi.org/10.1007/s00466-016-1266-2

[3] Wang, H., Al-Qadi, I. L. "Importance of nonlinear anisotropic modeling of granular base for predicting maximum viscoelastic pavement responses under moving vehicular loading", Journal of Engineering Mechanics, 139(1), pp. 29–38, 2013.
https://doi.org/10.1061/(ASCE)EM.1943-7889.0000465

[4] Souza, F. V., Castro, L. S. "Effect of temperature on the mechanical response of thermo-viscoelastic asphalt pavements", Construction and Building Materials, 30, pp. 574–582, 2012.
https://doi.org/10.1016/j.conbuildmat.2011.11.048

[5] Huang, C.-W., Al-Rub, R. K. A., Masad, E. A., Little, D. N. "Three-dimensional simulations of asphalt pavement permanent deformation using a nonlinear viscoelastic and viscoplastic model", Journal of Materials in Civil Engineering, 23(1), pp. 56–68, 2011.
https://doi.org/10.1061/(ASCE)MT.1943-5533.0000022

[6] Souad, H., Ismail, M., Hichem, A., Noureddine, E. "Vibration Analysis of Viscoelastic FGM Nanoscale Plate Resting on Viscoelastic Medium Using Higher-order Theory", Periodica Polytechnica Civil Engineering, 65(1), pp. 255–275, 2021.
https://doi.org/10.3311/PPci.16010

[7] Rekik, A. "Rigorous Estimates for Effective Creep-coefficients of Microcracked Masonry Accounting for Cracks Interactions", Periodica Polytechnica Civil Engineering, 64(2), pp. 557–578, 2020.
https://doi.org/10.3311/PPci.14157

[8] Dong, Z., Ni, H. "Dynamic model and criteria indices of semi-rigid base asphalt pavement", International Journal of Pavement Engineering, 15(9), pp. 854–866, 2014.
https://doi.org/10.1080/10298436.2014.893322

[9] Snehasagar, G., Krishnanunni, C. G., Rao, B. N. "Dynamics of vehicle–pavement system based on a viscoelastic Euler–Bernoulli beam model", International Journal of Pavement Engineering, 21(13), pp. 1669-1682, 2020.
https://doi.org/10.1080/10298436.2018.1562189

[10] Darabi, M. K., Huang, C.-W., Bazzaz, M., Masad, E. A., Little, D. N. "Characterization and validation of the nonlinear viscoelastic-viscoplastic with hardening-relaxation constitutive relationship for asphalt mixtures", Construction and Building Materials, 216, pp. 648–660, 2019.
https://doi.org/10.1016/j.conbuildmat.2019.04.239

[11] Karimi, M. M., Darabi, M. K., Tabatabaee, N. "A thermodynamic-based large deformation viscoplastic constitutive relationship for asphalt concrete compaction", International Journal of Solids and Structures, 165, pp. 192–216, 2019.
https://doi.org/10.1016/j.ijsolstr.2019.01.016

[12] Zhu, H., Sun, L. "A viscoelastic–viscoplastic damage constitutive model for asphalt mixtures based on thermodynamics", International Journal of Plasticity, 40, pp. 81–100, 2013.
https://doi.org/10.1016/j.ijplas.2012.07.005

[13] Cui, Y., Chen, D., Feng, L., Wang, L. "Effects of salt freeze damage on the viscoelastic performance of asphalt mortar", Ceramics-Silikáty, 61(3), pp. 257–266, 2017.
https://doi.org/10.13168/cs.2017.0024

[14] Zbiciak, A., Brzeziński, K., Michalczyk, R. "Constitutive models of pavement asphaltic layers based on mixture compositions", Journal of Civil Engineering and Management, 23(3), pp. 378–383, 2017.
https://doi.org/10.3846/13923730.2015.1128483

[15] Xu, S., Zhu, H. "Prediction of rutting in asphalt pavements by using viscoelastic theory", Journal of Tongji University (Natural Science), 18(3), pp. 299–305, 1990. (in Chinese)

[16] Chun, S., Kim, K., Greene, J., Choubane, B. "Evaluation of inter-layer bonding condition on structural response characteristics of asphalt pavement using finite element analysis and full-scale field tests", Construction and Building Materials, 96, pp. 307–318, 2015.
https://doi.org/10.1016/j.conbuildmat.2015.08.031

[17] Yang, K., Li, R. "Characterization of bonding property in asphalt pavement interlayer: A review", Journal of Traffic and Transportation Engineering (English Edition), 8(3), pp. 374–387, 2021.
https://doi.org/10.1016/j.jtte.2020.10.005

[18] Guo, C., Wang, F., Zhong, Y. "Assessing pavement interfacial bonding condition", Construction and Building Materials, 124, pp. 85–94, 2016.
https://doi.org/10.1016/j.conbuildmat.2016.07.064

[19] Kaliske, M., Behnke, R., Hartung, F., Wollny, I. "Multi-physical and multi-scale theoretical-numerical modeling of tire-pavement interaction", In: Kaliske, M., Oeser, M., Eckstein, L., Leischner, S., Ressel, W., Wellner, F. (eds.) Coupled System Pavement - Tire - Vehicle, Springer, 2021, pp. 1–39. ISBN 978-3-030-75488-4
https://doi.org/10.1007/978-3-030-75486-0_1

[20] Assogba, O. C., Tan, Y., Zhou, X., Zhang, C., Anato, J. N. "Numerical investigation of the mechanical response of semi-rigid base asphalt pavement under traffic load and nonlinear tempera-ture gradient effect", Construction and Building Materials, 235, 117406, 2020.
https://doi.org/10.1016/j.conbuildmat.2019.117406

[21] Wang, X., Ma, X. "Responses of semi-rigid base asphalt pave-ment with interlayer contact bonding model", Advances in Civil Engineering, 2020, 8841139, 2020.
https://doi.org/10.1155/2020/8841139

[22] Xu, J., Li, N., Xu, T. "Temperature changes of interlaminar bond-ing layer in different seasons and effects on mechanical properties of asphalt pavement", International Journal of Pavement Research and Technology, 15, pp. 589–605, 2022.
https://doi.org/10.1007/s42947-021-00039-9

[23] Jiang, X., Zeng, C., Yao, K., Gu, H.-Y., Li, Z.-K., Qiu, Y.-J. "Influence of bonding conditions on flexible base asphalt pave-ment under non-uniform vertical loads", International Journal of Pavement Engineering, 22(12), pp. 1491–1503, 2021.
https://doi.org/10.1080/10298436.2019.1697441

[24] Ma, X., Quan, W., Dong, Z. "Analytical solution for dynamic response of transversely isotropic viscoelastic asphalt pavement", China Journal of Highway and Transport, 33(10), pp. 135–145, 2020. (in Chinese)
https://doi.org/10.19721/j.cnki.1001-7372.2020.10.008

[25] Rahman, A., Huang, H., Ai, C. "Effect of shear stresses on asphalt pavement performance and evaluating debonding potential under repeated loading: numerical study", Journal of Transportation Engineering, Part B: Pavements, 147(3), 04021023, 2021.
https://doi.org/10.1061/JPEODX.0000283

[26] Liao, G., Wang, H., Zhu, H., Sun, P., Chen, H. "Shear strength between poroelastic road surface and sublayer with different bonding agents", Journal of Materials in Civil Engineering, 30(3), 04018017, 2018.
https://doi.org/10.1061/(ASCE)MT.1943-5533.0002216

[27] Wu, S., Chen, H., Zhang, J., Zhang, Z. "Effects of interlayer bonding conditions between semi-rigid base layer and asphalt layer on mechanical responses of asphalt pavement structure", International Journal of Pavement Research and Technology, 10(3), pp. 274–281, 2017.
https://doi.org/10.1016/j.ijprt.2017.02.003

[28] Goodman, R. E., Taylor, R. L., Brekke, T. L. "A model for the mechanics of jointed rock", Journal of the Soil Mechanics and Foundations Division, 94(3), pp. 637–659, 1968.
https://doi.org/10.1061/JSFEAQ.0001133

[29] Deng, X., Li, C. "The stress of road structure under horizontal load", Chinese Journal of Geotechnical Engineering, 24(4), pp. 427–431, 2002. (in Chinese)

[30] Guo, D., Feng, D. "Mechanics of Layered Elastic Systems", Harbin Institute of Technology Press, 2001. (in Chinese) ISBN 7-5603-1616-6

[31] Huang, T., Zhong, S., Li, Z. "Matrix Theory", Higher Education Press, Beijing, 2003. (in Chinese) ISBN 7-04-011942-0

[32] Durbin, F. "Numerical inversion of Laplace transforms an efficient improvement to Dubner and Abate's method", The Computer Journal, 17(4), pp. 371–376, 1974.
https://doi.org/10.1093/comjnl/17.4.371

[33] Gao, Y., Wang, P., Jiao, Y., Liu, Z., Xiao, H. "Viscoelastic dynamic response of asphalt pavement with imperfect interface bonding base on transfer matrix", ZAMM-Journal of Applied Mathematics and Mechanics, 102(5), e202100176, 2022.
https://doi.org/10.1002/zamm.202100176